SUPPLEMENTARY INFORMATION

LptB-LptF coupling mediates closure of the substrate-binding cavity in the $LptB_2FGC$ transporter through a rigid-body mechanism to extract LPS

Running title: Coupling of ATPase function to LPS extraction in $LptB_2FGC$

Emily A. Lundstedt, Brent W. Simpson[†], and Natividad Ruiz[*]

Department of Microbiology, The Ohio State University, Columbus, OH 43210, USA

*For correspondence. E-mail ruiz.82@osu.edu; Tel. 614-292-3426; Fax 614-292-8120

[†]Present address: Department of Infectious Diseases, College of Veterinary Medicine, University of Georgia, Athens, Georgia, USA

Table S1: Strains used in this study.

Strain	Genotype	Source
DH5α	F^- φ80*lacZ*ΔM15 Δ(*lacZYA-argF*)U169 *recA1 endA1 hsdR17* (r_K^-, m_K^+) *phoA sup*E44 λ^- *thi*-1	Life Technologies
NR1414	NR754 (pET23/42)	(Sherman *et al.*, 2014)
NR754	MC4100 ara^+	(Ruiz *et al.*, 2006)
NR760	NR754 *lptD4213*	(Ruiz *et al.*, 2006)
NR4904	NR754 *lptD4213* Δ*lpxM::kan*	This study
NR3936	NR754 Δ*lptB* (pRC7KanLptB)	This study
NR2583	NR754 (pET23/42LptB)	(Simpson *et al.*, 2016)
NR4446	NR754 Δ*lptB* (pET23/42LptB)	This study
NR4805	NR754 (pET23/42LptB/E86A)	This study
NR5522	NR754 (pET23/42lptB/E86R)	This study
NR4978	NR754 Δ*lptB* (pET23/42LptB/E86Q)	This study
NR4923	NR754 Δ*lptB* (pET23/42LptB/E86D)	This study
NR4607	NR754 Δ*lptB* (pET23/42LptB/E86A; pRC7KanLptB)	This study
NR4979	NR754 Δ*lptB* (pET23/42LptB/E86R; pRC7KanLptB)	This study
NR4747	NR754 Δ*lptB* (pET23/42LptB/E86A; pRC7CatSacBLptB)	This study
NR4745	NR754 Δ*lptB yjgN::tet* (pET23/42LptB/E86A; pRC7KanLptB)	This study
NR5778	NR754 Δ*lptB* (pET23/42LptB/E86A/R144H; pRC7CatSacBLptB)	This study
NR3174	NR754 Δ*lptB tet2* (pET23/42LptB/R144H)	(Simpson *et al.*, 2019)
NR3032	NR754 Δ*lptB tet2* (pET23/42LptB/R144H-EHis8)	(Simpson *et al.*, 2019)
NR1896	NR754 Δ*lptB* (pET23/42LptB-EHis8)	(Simpson *et al.*, 2019)
NR5123	NR754 Δ*lptB* (pET23/42LptB/E86A-EHis8; pRC7KanLptB)	This study
NR5124	NR754 Δ*lptB* (pET23/42LptB/E86A/G236A; pRC7KanLptB)	This study
NR5125	NR754 Δ*lptB* (pET23/42LptB/E86A/F239A; pRC7KanLptB)	This study
NR5446	NR754 Δ*lptB* (pET23/42LptB/E86Q-EHis8)	This study
NR5447	NR754 Δ*lptB* (pET23/42LptB/E86Q/G236A; pRC7KanLptB)	This study
NR6069	NR754 Δ*lptB* (pET23/42LptB/E86Q/F239A)	This study
NR4855	NR754 Δ*lpxM::kan*	This study
NR4876	NR754 Δ*lpxL::kan*	This study
NR4887	NR754 Δ*lpxP::kan*	This study
NR5327	NR754 Δ*lpxM::frt*	This study
NR5328	NR754 Δ*lpxP::frt*	This study
NR5372	NR754 Δ*lpxM::frt* Δ*lpxP::kan*	This study
NR5373	NR754 Δ*lpxM::frt* Δ*lpxL::kan*	This study
NR5374	NR754 Δ*lpxP::frt* Δ*lpxL::kan*	This study
NR5521	NR754 Δ*lpxM::frt* Δ*lpxP::frt*	This study
NR5572	NR754 Δ*lpxM::frt* Δ*lpxP::frt* Δ*lpxL::kan*	This study
NR4868	NR754 Δ*lptB* Δ*lpxM::kan* (pRC7CatSacBLptB)	This study
NR4872	NR754 Δ*lptB* Δ*lpxL::kan* (pRC7CatSacBLptB)	This study
NR4888	NR754 Δ*lptB* Δ*lpxP::kan* (pRC7CatSacBLptB)	This study
NR4944	NR754 Δ*lptB* Δ*lpxM::frt* (pRC7CatSacBLptB)	This study
NR5448	NR754 Δ*lptB* Δ*lpxP::frt* (pRC7CatSacBLptB)	This study
NR4924	NR754 Δ*lptB* Δ*lpxM::frt* Δ*lpxP::kan* (pRC7CatSacBLptB)	This study

NR4925	NR754 Δ*lptB tet2* Δ*lpxM::frt* Δ*lpxL::kan (*pRC7CatSacBLptB	This study
NR5573	NR754 Δ*lptB tet2* Δ*lpxP::frt* Δ*lpxL::kan* (pRC7CatSacBLptB)	This study
NR5329	NR754 Δ*lptB* Δ*lpxM::frt* Δ*lpxP::frt* (pRC7CatSacBLptB)	This study
NR4988	NR754 Δ*lptB tet2* Δ*lpxM::frt* Δ*lpxP::frt* Δ*lpxL::kan* (pRC7CatSacBLptB)	This study
NR4728	NR754 Δ*lptB* Δ*lpxM::kan* (pET23/42LptB)	This study
NR4854	NR754 Δ*lptB* Δ*lpxM::kan* (pET23/42LptB/E86A)	This study
NR5458	NR754 Δ*lptB* Δ*lpxM::kan* (pET23/42LptB/E86Q)	This study
NR5457	NR754 Δ*lptB* Δ*lpxM::kan* (pET23/42LptB/E86D)	This study
NR6278	NR754 Δ*lptB* Δ*lpxM::kan (*pET/42LptB/E86R; pRC7CatSacBLptB)	This study
NR4940	NR754 Δ*lptB* Δ*lpxM::kan* (pET23/42LptB/R144H)	This study
NR5779	NR754 Δ*lptB* Δ*lpxM::kan* (pET23/42LptB/E86A/R144H; pRC7CatSacBLptB)	This study
NR4932	NR754 Δ*lptB* Δ*lpxM::kan* (pET23/42LptB-EHis8; pRC7CatSacBLptB)	This study
NR4877	NR754 Δ*lptB* Δ*lpxL::kan* (pET23/42LptB)	This study
NR5900	NR754 Δ*lptB* Δ*lpxL::kan* (pET23/42LptB/E86Q)	This study
NR5973	NR754 Δ*lptB* Δ*lpxL::kan* (pET23/42LptB/E86A)	This study
NR4933	NR754 Δ*lptB* Δ*lpxL::kan* (pET23/42LptB/E86A; pRC7CatSacBLptB)	This study
NR5972	NR754 Δ*lptB* Δ*lpxL::kan* (pET23/42LptB/R144H)	This study
NR4889	NR754 Δ*lptB* Δ*lpxP::kan* (pET23/42LptB)	This study
NR5971	NR754 Δ*lptB* Δ*lpxP::kan* (pET23/42LptB/E86Q)	This study
NR4947	NR754 Δ*lptB* Δ*lpxP::kan* (pET23/42LptB/E86A; pRC7CatSacBLptB)	This study
NR5970	NR754 Δ*lptB* Δ*lpxP::kan* (pET23/42LptB/R144H)	This study
NR4980	NR754 Δ*lptB* Δ*lpxM::frt* Δ*lpxP::kan* (pET23/42LptB)	This study
NR5974	NR754 Δ*lptB* Δ*lpxM::frt* Δ*lpxP::kan* (pET23/42LptB/E86Q)	This study
NR4981	NR754 Δ*lptB* Δ*lpxM::frt* Δ*lpxP::kan* (pET23/42LptB/E86A)	This study
NR4982	NR754 Δ*lptB* Δ*lpxM::frt* Δ*lpxP::kan* (pET23/42LptB/R144H)	This study
NR4984	NR754 Δ*lptB tet2* Δ*lpxM::frt* Δ*lpxL::kan* (pET23/42LptB)	This study
NR5975	NR754 Δ*lptB tet2* Δ*lpxM::frt* Δ*lpxL::kan* (pET23/42LptB/E86Q)	This study
NR4986	NR754 Δ*lptB tet2* Δ*lpxM::frt* Δ*lpxL::kan* (pET23/42LptB/R144H)	This study
NR4985	NR754 Δ*lptB tet2* Δ*lpxM::frt* Δ*lpxL::kan* (pET23/42LptB/E86A)	This study
NR4975	NR754 Δ*lptB tet2* Δ*lpxP::frt* Δ*lpxL::kan* (pET23/42LptB)	This study
NR6141	NR754 Δ*lptB tet2* Δ*lpxP::frt* Δ*lpxL::kan* (pET23/42LptB/E86Q)	This study
NR4976	NR754 Δ*lptB tet2* Δ*lpxL::frt* Δ*lpxP::kan* (pET23/42LptB/E86A)	This study
NR4977	NR754 Δ*lptB tet2* Δ*lpxL::frt* Δ*lpxP::kan* (pET23/42LptB/R144H)	This study
NR6142	NR754 Δ*lptB tet2* Δ*lpxM::frt* Δ*lpxP::frt* Δ*lpxL::kan* (pET23/42LptB)	This study
NR6143	NR754 Δ*lptB tet2* Δ*lpxM::frt* Δ*lpxP::frt* Δ*lpxL::kan* (pET23/42LptB/E86Q)	This study
NR6145	NR754 Δ*lptB tet2* Δ*lpxM::frt* Δ*lpxP::frt* Δ*lpxL::kan* (pET23/42LptB/R144H)	This study
NR6144	NR754 Δ*lptB tet2* Δ*lpxM::frt* Δ*lpxP::frt* Δ*lpxL::kan* (pET23/42LptB/E86A)	This study
NR2759	NR754 Δ*lptFG* (pRC7KanLptFG)	(Simpson *et al.*, 2016)
NR4973	NR754 Δ*lptFG* Δ*lpxM::frt* (pRC7KanLptFG)	This study
NR2761	NR754 Δ*lptFG* (pBAD18LptFG3)	(Simpson *et al.*, 2016)
NR3079	NR754 (pBAD18LptFG3)	(Simpson *et al.*, 2016)
NR4831	NR754 *yjgN::tet* Δ*lptB* (pET23/42LptB)	This study
NR3265	NR754 Δ*lptFG* (pBAD18LptFG3/LptF/E84A)	(Simpson *et al.*, 2016)
NR2762	NR754 Δ*lptFG* (pBAD18LptFG3/LptG/E88A)	(Simpson *et al.*, 2016)

NR3327	NR754 Δ*lptFG* (pBAD18LptFG3/LptF/E84A/LptG/E88A)	(Simpson *et al*., 2016)
NR5036	NR754 Δ*lptFG* Δ*lpxM::frt* (pBAD18LptFG3/LptF/E84A)	This study
NR5037	NR754 Δ*lptFG* Δ*lpxM::frt* (pBAD18LptFG3/LptG/E88A)	This study
NR5038	NR754 Δ*lptFG* Δ*lpxM::frt* (pBAD18LptFG3/LptF/E84A/LptG/E88A)	This study
NR3740	NR754 Δ*lptFG* (pBAD18LptFG3/LptG/K34A)	(Bertani *et al*., 2018)
NR5575	NR754 Δ*lptFG* Δ*lpxM::frt* (pBAD18LptFG3/LptG/K34A)	This study
NR6340	NR754 Δ*lptFG* (pBAD18LptFG3/LptF/E84A/LptG/A110V)	This study
NR6341	NR754 Δ*lptFG* (pBAD18LptFG3/LptG/E88A/A110V)	This study
NR6342	NR754 Δ*lptFG* (pBAD18LptFG3/LptF/E84A/LptG/E88A/A110V)	This study
NR6343	NR754 Δ*lptFG* (pBAD18LptFG3/LptF/E84A/LptG/L74P)	This study
NR6344	NR754 Δ*lptFG* (pBAD18LptFG3/LptG/L74P/E88A)	This study
NR6345	NR754 Δ*lptFG* (pBAD18LptFG3/LptF/E84A/LptG/L74P/E88A)	This study
NR3259	NR754 Δ*lptFG* (pBAD18LptFG3/LptF/S83A)	(Simpson *et al*., 2016)
NR6338	NR754 Δ*lptFG* (pBAD18LptFG3/LptF/S83A/LptG/S87A)	This study
NR6339	NR754 Δ*lptFG* (pBAD18LptFG3/LptG/S87A)	This study
NR4126	NR754 *yjgN::tet*	This study
NR6048	NR754 *yjgN::tet lptGL74P*	This study
NR6049	NR754 *yjgN::tet lptGL74P* Δ*lptB* (pRC7KanLptB)	This study
NR6071	NR754 *yjgN::tet lptGL74P* Δ*lptB* (pET23/42LptB)	This study
NR6072	NR754 *yjgN::tet lptGL74P* Δ*lpxM::kan*	This study
NR6073	NR754 *yjgN::tet lptGL74P* Δ*lptB* (pET23/42LptB/E86A)	This study
NR6074	NR754 *yjgN::tet lptGL74P* Δ*lptB* (pET23/42LptB/E86Q)	This study
NR6075	NR754 *yjgN::tet lptGL74P* Δ*lptB* (pET23/42LptB/R144H)	This study
NR6077	NR754 *yjgN::tet lptGL74P* Δ*lptB* (pET23/42LptB-EHis8; pRC7KanLptB)	This study
NR6328	NR754 *yjgN::tet* Δ*lpxM::kan*	This study
NR6329	NR754 Δ*lptFG* (pBAD18LptFG3/LptG/L74P)	This study
NR6330	NR754 Δ*lptFG* (pBAD18LptFG3/LptG/A110V)	This study
NR5065	NR754 *yjgN::tet lptGA110V*	This study
NR5406	NR754 *yjgN::tet lptGA110V* Δ*lptB* (pRC7KanLptB)	This study
NR5425	NR754 *yjgN::tet lptGA110V* Δ*lptB* (pRC7KanLptB; pET23/42LptB/R144H)	This study
NR5427	NR754 *yjgN::tet lptGA110V* Δ*lptB* (pRC7KanLptB; pET23/42LptB-EHis8)	This study
NR5464	NR754 *yjgN::tet lptGA110V* Δ*lpxM::kan*	This study
NR5479	NR754 *yjgN::tet lptGA110V* Δ*lptB* (pET23/42LptB)	This study
NR5485	NR754 *yjgN::tet lptGA110V* Δ*lptB* (pET23/42LptB/E86Q)	This study
NR5492	NR754 *yjgN::tet lptGA110V* Δ*lptB* (pET23/42LptB/E86A)	This study

Table S2: Primers used in this study.

Primer Name	Sequence (5'-3')
LptBE86Asense	CTATCTGCCACAGGCTGCCTCCATTTTCCG
LptBE86Aanti	CGGAAAATGGAGGCAGCCTGTGGCAGATAG
LptBE86DFwd	TATCTGCCACAGGATGCCTCCATTTTC
LptBE86DRev	GAAAATGGAGGCATCCTGTGGCAGATA
LptBE86QFwd	TATCTGCCACAGCAACCTCCATTTTCC
LptBE86QRev	GGAAAATGGAGGTTGCTGTGGCAGATA
LptBE86RFwd	TATCTGCCACAGAGACCTCCATTTTCC
LptBE86RRev	GGAAAATGGAGGTCTCTGTGGCAGATA
LptBG236Asense	GCGTGTATACCTTGCAGAAGACTTCAGACTC
LptBG236Aanti	GAGTCTGAAGTCTTCTGCAAGGTATACACGC
LpxMFwd	GTACGCAGTCAGTACCGGCTTTTTTTA
LpxMRev	TCCGGCCTACAGTTCAATGATAGTTCA
LpxLFwd	CAATTTCGCCCAGTCTTCAGCCAC
LpxLRev	CGCAATCCAGAGAGCTTTTATCGC
LpxPFwd	CAGGAACCATTGTCGTACATGATG
LpxPRev	CATGAGGTTATTATGGCCGATTTG
LptGA110VFwd	AAAACCGTAATTCCGCTGGTCTTGCTGACG
LptGA110VRev	CGGAATTACGGTTTTCATCACCGACAGCGC
5LptGL74P	GCTCTGCCTGGGGCGTTGCTTGGTCTTGGG
3LptGL74P	CGCCCCAGGCAGAGCCGCCATCGGGAAGAA
5lptF79UP	TCAAGAGAATAAATGACGTTTAAGCC
3lptG226DWN	GCCAAGTGACGAATCAGATTG
LptGS87AFwd	GCGCAGCGCGCAGAACTGGTGGTGATGCAGGC
LptGS87ARev	CACCAGTTCTGCGCGCTGCGCCAGCATCCCAAG

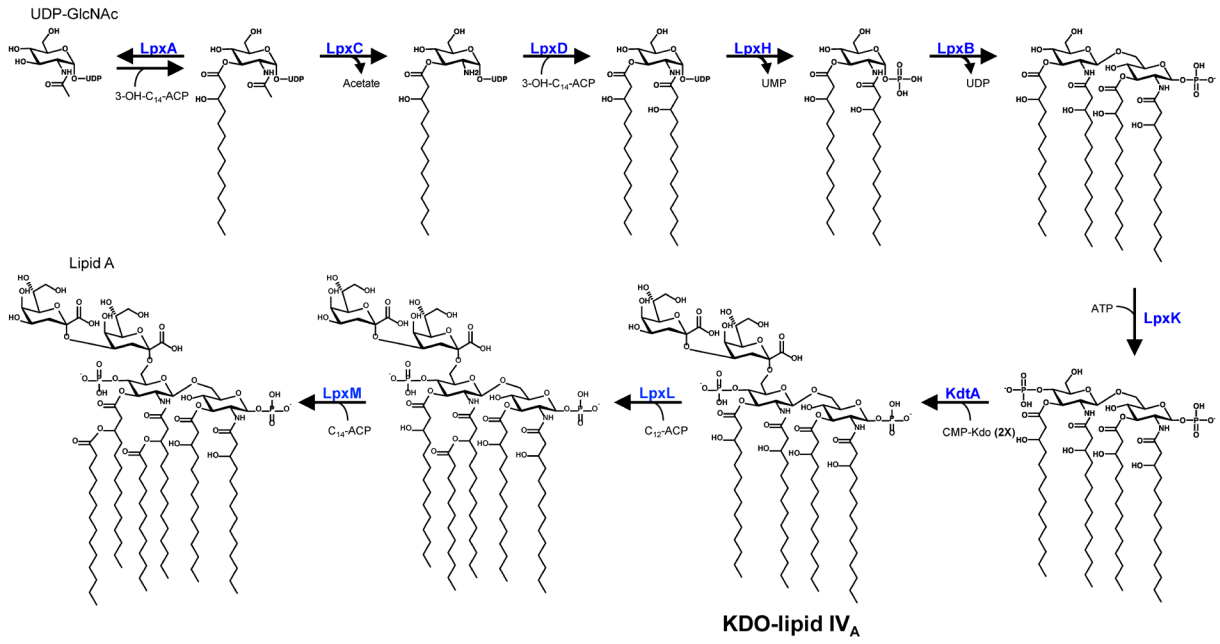

Figure S1: The Raetz pathway. The Raetz pathway for lipid A biosynthesis. Enzyme names are colored blue.

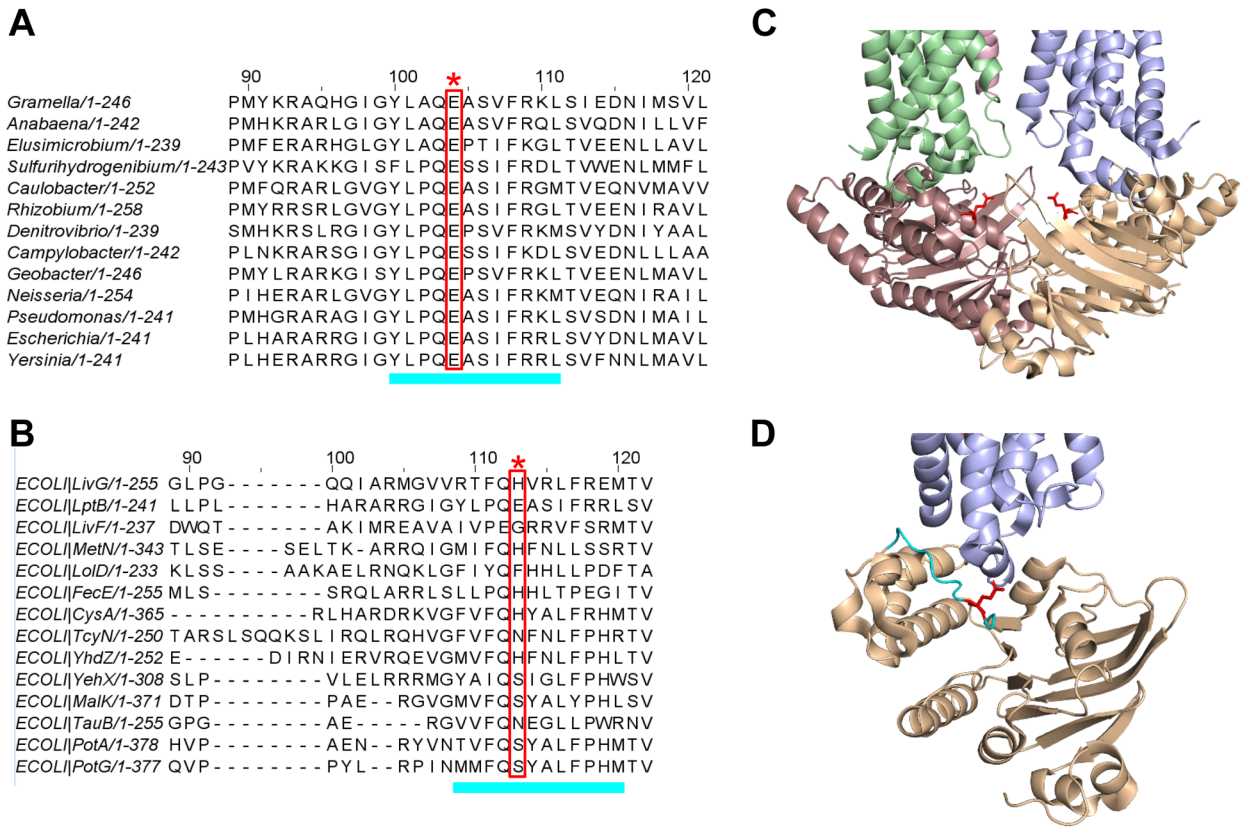

Figure S2: Conservation of residue E86 of LptB. Residue E86 of LptB is conserved across diverse species of gram-negative bacteria but not conserved in NBDs of other ABC transporters. **A)** A Clustal Omega alignment of LptB amongst different classes of gram-negative bacteria (Sievers *et al.*, 2011). Representative organisms were chosen based on the species sampled in Simpson et al. (2016). The following Uniprot accession numbers were used: *Gramella forsetii* (A0LYX6), *Anabaena variabilis* (Q3MCM5), *Elusimicrobium minutum* (B2KC16), *Sulfurihydrogenibium azorense* (C1DWB4), *Caulobacter vibrioides* (A0A0H3CCX7), *Rhizobium leguminosarum (*A0A179C0Q1*), Denitrovibrio acetiphilus* (D4H7T1), *Campylobacter jejuni* (A0A1E7NI33), *Geobacter uraniireducens* (A5G5S7), *Neisseria meningitidis* (A1KVS8), *Pseudomonas aeruginosa* (A0A071L2Z5), *Escherichia coli* (P0A9V1), and *Yersinia pestis* (A0A384L7T7). The equivalent residue to E86 in *E. coli* LptB is indicated by the red box and asterisk. The Q loop motif is marked by the cyan bar. **B)** An alignment of NBDs of other *E. coli* ABC transporters generated using Clustal Omega (Sievers *et al.*, 2011). The following Uniprot accession numbers were used: LivG (P0A9S7), LptB (P0A9V1), LivF (P22731), MetN

(P30750), LolD (P75957), FecE (P15031), CysA (P16676), TcyN (37774), YhdZ (P45769), YehX (P33360), MalK (P68187), TauB (Q47538), PotA (P69874), and PotG (P31134). The equivalent residue to E86 in *E. coli* LptB is indicated by the red box and asterisk. **C)** Section of the crystal structure of *Vibrio cholerae* $LptB_2FGC$ (PDB 6MJP) showing $LptB_2$ (monomers shown in brown and gold) interacting with the coupling helices of LptF (green) and LptG (light blue). Residue E86 is shown as red sticks in each LptB monomer. **D)** Side view of the structure from (**C**) showing an LptB monomer interacting with LptG. LptB residue E86 is shown as red sticks and the Q loop is colored cyan.

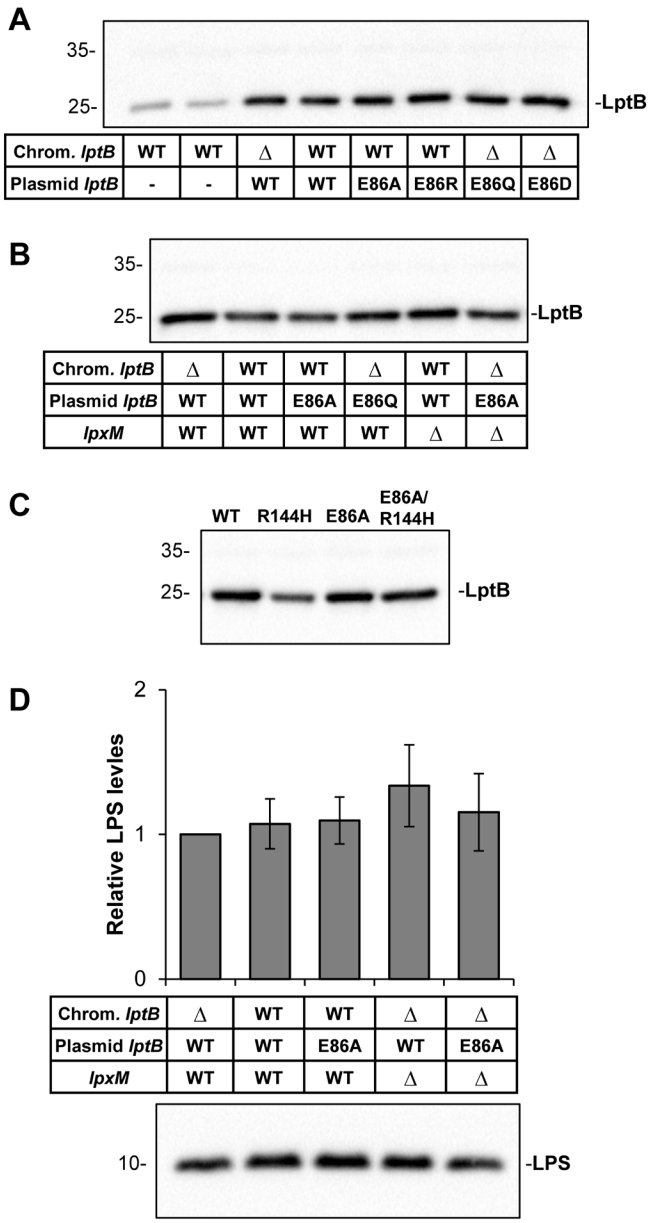

Figure S3: Substituting residue E86 in LptB does not affect levels of LptB or LPS. **A)** LptB immunoblot showing no difference in levels between $LptB^{E86}$ variants and $LptB^{WT}$. Note that pET23/42LptB produces higher levels of $LptB^{WT}$ than the chromosomal *lptB* allele. All blots shown are representative of at least three independent experiments. Numbers to the left of the blots indicate the band size in kDa. Strain NR4446 was used as the parental wild-type *lptB* strain. **B)** Δ*lpxM* does not suppress defective *lptB(E86)* alleles by altering the levels of LptB. Immunoblot assay of LptB levels comparing *lptB* mutants combined with Δ*lpxM.* NR4446 was used as the parent strain with wild-type *lptB*

and *lpxM* alleles. **C)** The double mutant pET23/42LptB/E86A/R144H does not complement a chromosomal *lptB* deletion, but does not alter the levels of LptB. The LptB E86A/R144H variant is not suppressed by Δ*lpxM*. Immunoblot comparing LptB levels in wild type and *lptB* mutants. WT refers to strain NR4446. **D)** Δ*lpxM* does not suppress *lptB(E86A)* by altering the levels of LPS in the cell. LPS levels were monitored by immunoblot and the intensity of the LPS band was quantified. Data shown represents the relative levels of LPS as determined by the ratio of the intensity of the LPS band from each sample with respect to that of the sample from the wild-type strain NR4446. Data represent the average of three independent experiments with error bars showing the standard deviation. A representative immunoblot is also shown.

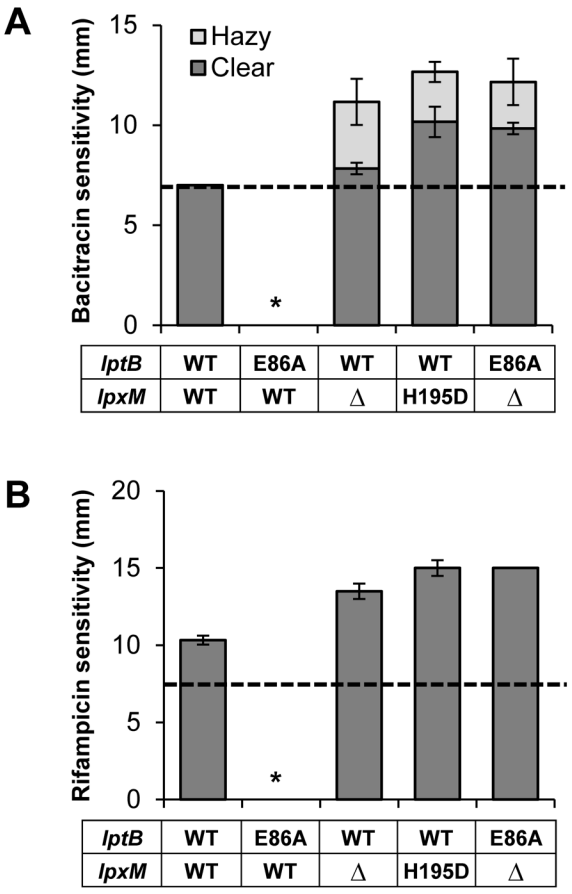

Figure S4: *lpxM(H195D)* is a total-loss-of-function allele. The original suppressor allele, *lpxM(H195D)*, shows equivalent suppression of *lptB(E86A)* as a deletion of *lpxM*. Thus *lpxM(H195D)* is a total-loss-of-function allele that is phenotypically equivalent to Δ*lpxM*. OM permeability was measured by sensitivity to bacitracin (panel) and rifampicin (panel **B**) via disc diffusion assay on LB plates. The dashed line represents the diameter of the antibiotic discs. The diameter of complete clearing (dark bars) and partial clearing (light bars) around the antibiotic disc is shown. The single *lptB(E86A)* mutant is not viable and is indicated by the asterisk. Data represent the average of three independent experiments with the error bars showing the standard deviation. No error bar indicates a standard deviation value of 0. WT refers to strain NR4446.

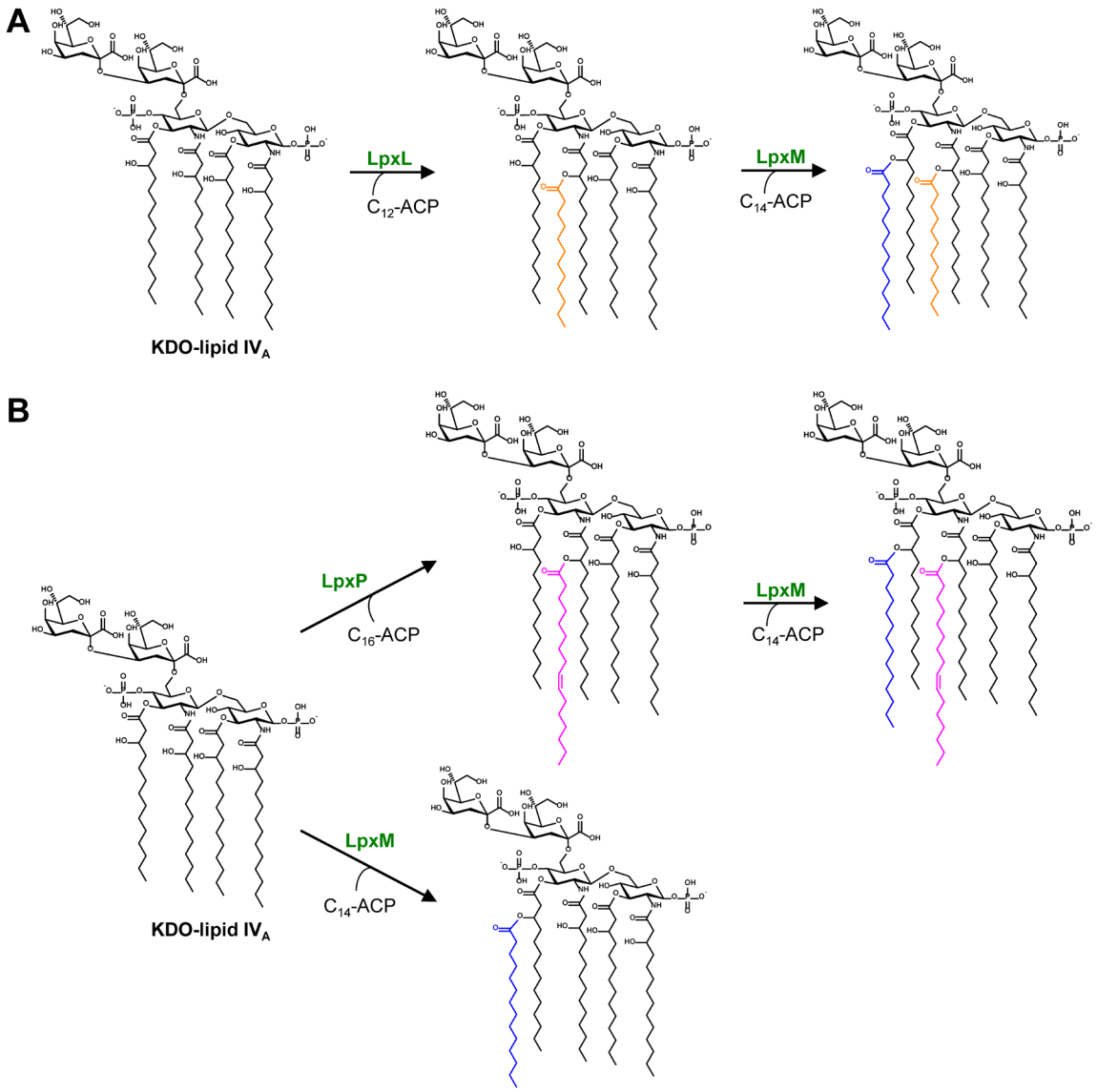

Figure S5: Canonical and alternative pathways for lipid A biosynthesis. Starting with lipid IV_A, the acylation steps catalyzed by different acyltransferase enzymes are shown. Acyl chains added by LpxM are colored blue, those added by LpxP are pink, and those added by LpxL are orange. **A)** The canonical pathway for lipid A biosynthesis present in wild-type cells grown at 30°C as shown in Vorachek-warren, Ramirez et al. (2002). LpxL adds a lauroyl group to the 2′-hydroxymyristoyl, then LpxM adds a myristoyl group to the 3′-hydroxymyristoyl group. **B)** At low temperatures or in the absence of LpxL, LpxP adds a palmitoleoyl group to the 2′-hydroxymyristoyl; then, the product is acylated by LpxM. In the absence of LpxL, LpxM is also able to use lipid IV_A as a substrate to add on the myristoyl group, but LpxP cannot use the resulting penta-acylated product as a substrate.

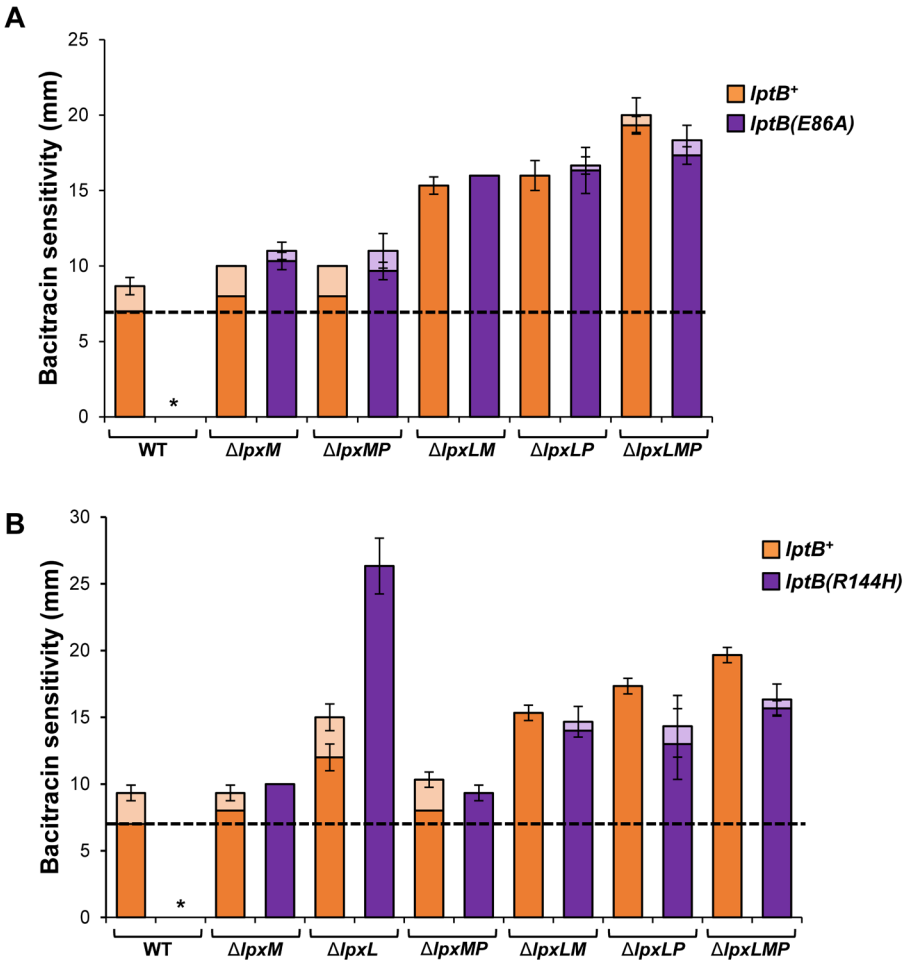

Figure S6: *lptB(E86A)* and *lptB(R144H)* are suppressed by *lpx* null alleles. OM permeability defects in the haploid *lptB(E86A)* (panel **A**) and *lptB(R144H)* (panel **B**) mutants are suppressed by the loss of lipid A acyltransferases. In these haploid strains, *lptB* alleles were encoded in pET23/42/LptB, pET23/42/LptB/E86A (shown in **A**), and pET23/42/LptB/R144H (shown in **B**). OM permeability was assessed by determining sensitivity to bacitracin using a disc diffusion assay on LB plates. Asterisks indicate that strains are unable to grow on LB. Any combinations of *lpx* null alleles that do not suppress these mutant *lptB* alleles are also not able to grow, so they are not shown. Clear and hazy zones around the disc are shown in dark and light colored bars respectively. Data shown are representative of at least three independent experiments. The diameter of the bacitracin disc is indicated with the dashed line. Data represent the average of three independent experiments with the error bars indicating the standard deviation. No error bar indicates a standard deviation value of 0. WT refers to strain NR4446.

A

	Phenotype
lptG(L74P)	Functional
lptG(A110V)	Partial LOF
lptB(R144H)	Conditional LOF
lptB(R144H) lptG(L74P)	Partial LOF
lptB(R144H) lptG(A110V)	Conditional LOF

B

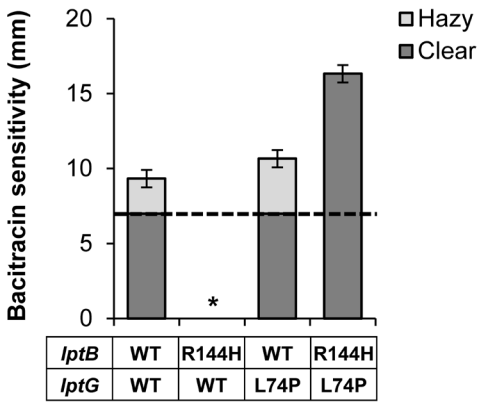

C

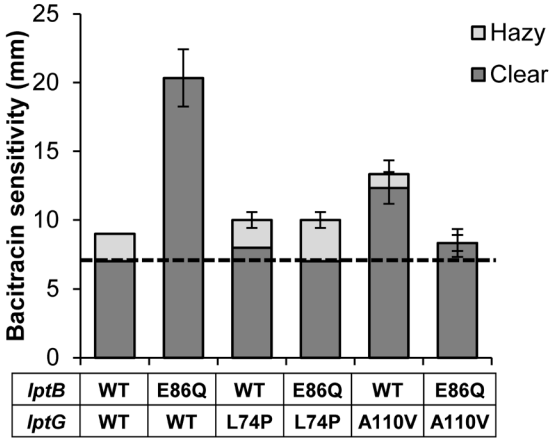

Figure S7: Analysis of suppression by *lptG(L74P)* and *lptG(A110V)* of defects caused by *lptB(E86Q*) and *lptB(R144H*). A) *lptB(R144H)* is suppressed by *lptG(L74P)* but not *lptG(A110V).* Plasmid-borne *lptB(R144H)* allele was assessed for its ability to complement chromosomal Δ*lptB* in strains carrying chromosomal *lptG*$^{+}$, *lptG(L74P)* or *lptG(A110V)* alleles. Table summarizes the results of the *lptB(R144H)* complementation tests. Functional refers to substitutions that confer no defects, partial LOF (loss of function) refers to those that confer OM-permeability defects, conditional LOF refers to those that prevent complementation of chromosomal Δ*lptB* in LB but not in minimal

media, and total LOF refers to those that do not complement chromosomal Δ*lptB* under any condition tested. **B)** *lptB(R144H)* is suppressed by *lptG(L74P)*. OM permeability was assessed by measuring the sensitivity to bacitracin on LB plates. Data shown are the average of three independent experiments with the error bars representing the standard deviation. The diameter of the disc containing bacitracin is indicated by the dashed line. The single *lptB(R144H)* mutant is not viable and is indicated by the asterisk. **C)** *lptB(E86Q)* is suppressed by both *lptG(L74P)* and *lptG(A110V).* Plasmid-borne *lptB(E86Q)* allele was assessed for its ability to complement chromosomal Δ*lptB* in strains carrying chromosomal *lptG*$^{+}$, *lptG(L74P)* or *lptG(A110V)*. All combinations complemented and their OM permeability was determined by disc diffusion assay. Data represent the average of three independent experiments with the error bars indicating the standard deviation. No error bar indicates a standard deviation value of 0. NR4831 was used as the parental wild-type *lptB lptG* strain.

A

	Phenotype
lptG(L74P)	Functional
lptG(A110V)	Partial LOF
lptB-EHis$_8$	Partial LOF
lptB-EHis$_8$ lptG(L74P)	Total LOF
lptB-EHis$_8$ lptG(A110V)	Conditional LOF

B

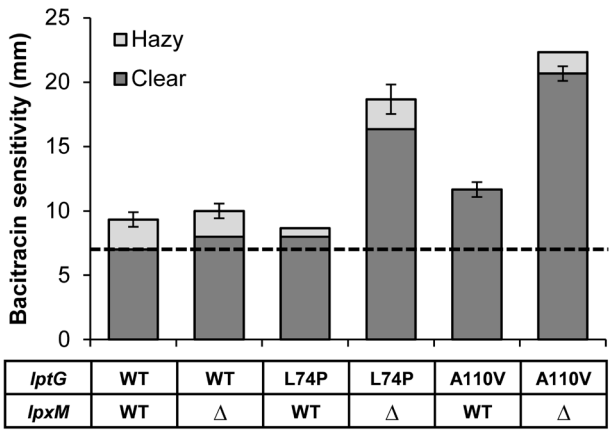

Figure S8: *lptG(L74P)* and *lptG(A110V)* are synthetic defective with *lptB-EHis$_8$* and Δ*lpxM*. A) *lptG(L74P)* and *lptG(A110V)* are synthetic lethal with the *lptB-EHis$_8$* allele. Plasmid-borne *lptB-EHis$_8$* was assessed for its ability to complement chromosomal Δ*lptB* in strains carrying chromosomal *lptG*$^+$, *lptG(L74P)* or *lptG(A110V)*. Table summarizing the complementation results. Functional refers to substitutions that confer no defects, partial LOF (loss of function) refers to those that confer OM-permeability defects, conditional LOF refers to those that prevent complementation of chromosomal Δ*lptB* in LB but not in minimal media, and total LOF refers to those that do not complement chromosomal Δ*lptB* under any condition tested. **B)** *lptG(L74P)* and *lptG(A110V)* are synthetic defective with Δ*lpxM*. Chromosomal *lpxM* gene was deleted in strains with chromosomal *lptG*$^+$, *lptG(L74P)* or *lptG(A110V)* alleles. OM-permeability defects were determined by assessing sensitivity to bacitracin using a disc diffusion assays. Dark bars represent zones of complete clearing, light bars represent zones of partial clearing around the disc. The dashed line indicates the diameter of the bacitracin disc. Data represent the average of three independent experiments with the error bars indicating the standard deviation. No error bar indicates a standard deviation value of 0. Strain NR4831 was used as the parental wild-type *lptB lptG* strain.

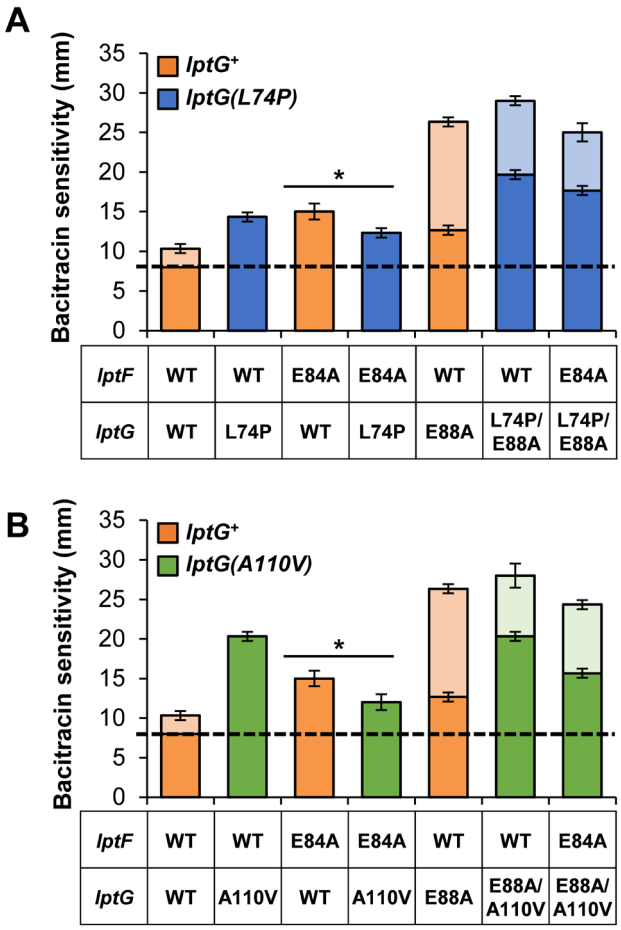

Figure S9: *lptG(L74P)* and *lptG(A110V)* only suppress defects in the coupling helix of LptF. A) *lptG(L74P)* suppresses *lptF(E84A)* alone or in combination with *lptG(E88A).* **B)** *lptG(A110V)* suppresses *lptF(E84A)* alone or in combination with *lptG(E88A)*. Haploid strains carrying alleles with substitutions in the conserved glutamates of the coupling helices [*lptF(E84A)*, *lptG(E88A)*, and *lptF(E84A) lptG(E88A)*] were each combined with either *lptG(L74P)* (**A**) or *lptG(A110V)* **(B**). All *lptFG* alleles were encoded in the pBAD18LptFG3 plasmid and the chromosomal wild-type *lptFG* alleles were deleted. OM permeability of these strains was assessed via disc diffusion assay measuring sensitivity to bacitracin on LB plates. Clear zones around the disc are shown in darker colored bars, hazy zones around the disc are shown in lighter colored bars. Disc diameter indicated by the dashed line. Since the double mutant *lptF(E84A) lptG(E88A)* does not complement on LB, it is not shown. Data represent the average of three independent experiments. The error bars show the standard deviation. Strain NR2761 was used as the parental wild-

type *lptFG* strain. An unpaired two-tailed Student's *t*-test was used to assess the significance of difference between *lptF(E84A)* and *lptF(E84A)* combined with either *lptG(L74P)* or *lptG(A110V)*. * indicates $P < 0.05$.

REFERENCES

Bertani, B.R., Taylor, R.J., Nagy, E., Kahne, D., and Ruiz, N. (2018) A cluster of residues in the lipopolysaccharide exporter that selects substrate variants for transport to the outer membrane. *Molecular Microbiology* **109**: 541-554.

Ruiz, N., Wu, T., Kahne, D., and Silhavy, T.J. (2006) Probing the barrier function of the outer membrane with chemical conditionality. *ACS Chemical Biology* **1**: 385-395.

Sherman, D.J., Lazarus, M.B., Murphy, L., Liu, C., Walker, S., Ruiz, N., and Kahne, D. (2014) Decoupling catalytic activity from biological function of the ATPase that powers lipopolysaccharide transport. *Proceedings of the National Academy of Sciences of the United States of America* **111**: 4982-4987.

Sievers, F., Wilm, A., Dineen, D., Gibson, T.J., Karplus, K., Li, W., Lopez, R., McWilliam, H., Remmert, M., Soding, J., Thompson, J.D., and Higgins, D.G. (2011) Fast, scalable generation of high-quality protein multiple sequence alignments using Clustal Omega. *Molecular Systems Biology* **7**: 539.

Simpson, B.W., Owens, T.W., Orabella, M.J., Davis, R.M., May, J.M., Trauger, S.A., Kahne, D., and Ruiz, N. (2016) Identification of residues in the lipopolysaccharide ABC transporter that coordinate ATPase activity with extractor function. *mBio* **7**: 13-17.

Simpson, B.W., Pahil, K.S., Owens, T.W., Lundstedt, E.A., Davis, R.M., Kahne, D., and Ruiz, N. (2019) Combining mutations that inhibit two distinct steps of the ATP hydrolysis cycle restores wild-type function in the lipopolysaccharide transporter and shows that ATP binding triggers transport. *mBio* **10**: 1-18.